

Radiological approach to COVID-19 pneumonia with an emphasis on chest CT

Serkan Güneyli 
Zeynep Atçeken 
Hakan Doğan 
Emre Altınmakas 
Kayhan Çetin Atasoy 

ABSTRACT

Coronavirus disease 2019 (COVID-19) has recently become a worldwide outbreak with several millions of people infected and more than 160 000 deaths. A fast and accurate diagnosis in this outbreak is critical to isolate and treat patients. Radiology plays an important role in the diagnosis and management of the patients. Among various imaging modalities, chest CT has received attention with its higher sensitivity and specificity rates. Shortcomings of the real-time reverse transcriptase-polymerase chain reaction test, including inappropriate sample collection and analysis methods, initial false negative results, and limited availability has led to widespread use of chest CT in the diagnostic algorithm. This review summarizes the role of radiology in COVID-19 pneumonia, diagnostic accuracy of imaging, and chest CT findings of the disease.

COVID-19, which appeared first in Wuhan, Hubei, China, has rapidly extended worldwide and become an outbreak (1). The main routes of transmission include inhalation of respiratory droplets and contact with contaminated surfaces (2–4). The most common symptoms of the disease are fever and dry cough, but it may present with various clinical findings, e.g., fatigue, myalgia, gastrointestinal, and nervous system symptoms (5–8). The disease may progress fast and lead to death especially in the elderly and patients with chronic diseases. It is diagnosed mainly from epidemiologic factors, clinical manifestations, chest computed tomography (CT) findings, and nucleic acid detection of the virus (1).

The gold standard method in the diagnosis of COVID-19 is real-time reverse transcriptase-polymerase chain reaction (rRT-PCR) test (9, 10). However, initial rRT-PCR test may be negative because of inappropriate sample collection and laboratory analysis (11). Notwithstanding the necessity of a fast and accurate diagnosis required to isolate and manage the patients optimally, the sensitivity of the rRT-PCR test has been found to vary widely. Thus, in settings where the availability, turnaround times, and accuracy of rRT-PCR test impose limitations for the virologic diagnosis, imaging, especially chest CT, has played an important role in the diagnosis as well as in the management of the disease (12, 13). Chest X-ray, ultrasound, magnetic resonance imaging (MRI), 18F-fluorodeoxyglucose positron emission tomography/CT are among the other imaging modalities used so far in the management of COVID-19 pneumonia (1, 7, 14–17).

We identified a total of 11 published articles about COVID-19 pneumonia with a sample size of more than 50 patients (1, 5, 18–26) and reviewed the role of radiology and CT findings in COVID-19 pneumonia.

Chest X-ray

Chest X-ray, particularly with portable equipment, may be used in COVID-19 pneumonia as the first imaging modality with the advantages of less ionizing radiation compared with CT, ease of sterilization of the equipment, and rapid application in outpatient suites and wards without a need of transferring the patients to the radiology department (15). Heavy use of CT for COVID-19 diagnosis and management may decrease the use of CT for routine non-COVID purposes. Also, the CT room and equipment carry a risk of being contaminated and becoming vectors for cross-infection of the radiology personnel and other patients, if optimal precau-

From the Department of Radiology (S.G.✉
drserkanguneli@gmail.com), Koc University School
of Medicine, Istanbul, Turkey

Received 21 April 2020; accepted 22 April 2020.

Published online 30 April 2020.

DOI 10.5152/dir.2020.20260

You may cite this article as: Güneyli S, Atçeken Z, Doğan H, Altınmakas E, Atasoy KÇ. Radiological approach to COVID-19 pneumonia with an emphasis on chest CT. Diagn Interv Radiol 2020; 26:323–332.

tions are not taken. Thus, American College of Radiology suggested that portable chest X-ray may be considered to minimize the risk of disease spread and decrease the burden on the radiology departments (27). Some institutions have used chest X-ray as a first-line triage tool in this outbreak (15). However, the sensitivity of chest X-ray ranges between 33%–69%, not remarkably higher than that of the rRT-PCR test (28). On the other hand, chest CT was reported to have much higher sensitivity compared with that of chest X-ray (15, 29). Chest X-ray is insensitive in mild or early stages of COVID-19 infection, therefore it is generally not recommended as a screening method in COVID-19 pneumonia (Fig. 1a). Radiographic findings of COVID-19 pneumonia include consolidations or hazy opacities, which are often bilateral and peripheral (Fig. 1b–d).

Chest X-ray may be useful in the diagnosis of other diseases that may mimic COVID-19 pneumonia, such as lobar pneumonia due to bacterial infections, pulmonary edema, pneumothorax, and pleural effusion. It may also be used as a first-line imaging method in young and pregnant patients, owing to its low radiation dose. Chest X-ray may be helpful in hospitalized patients to evaluate the progression of the disease (30), though it was found that daily chest X-rays had no added value in the management of stable patients with COVID-19, and unnecessary X-rays should be avoided to minimize the risk of spread (30). Since CT is more sensitive for early pneumonic changes, it may be employed to detect disease if the clinical suspicion is high but the ra-

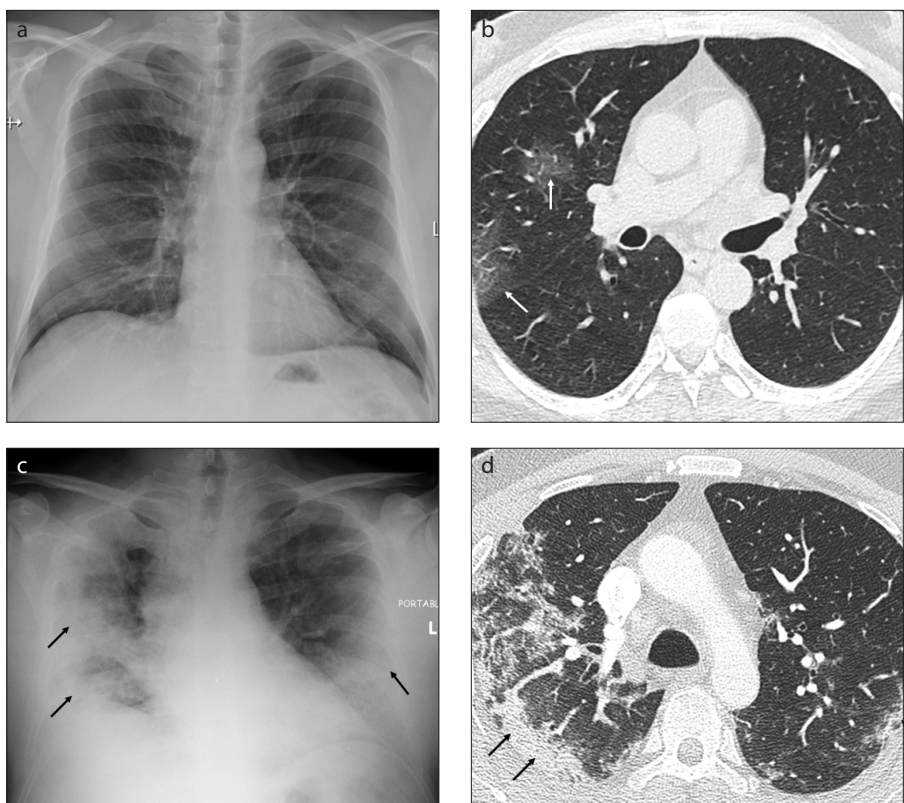


Figure 1. a–d. In this example, initial chest X-ray was negative (a). Two days later, axial CT image (b) displays two foci of GGO (arrows) in the right lung. Nine days later, chest X-ray image (c) shows bilateral peripheral consolidations (arrows). On day 16, axial CT image (d) shows bilateral peripheral consolidations (arrows).

diography is normal, for a timely isolation and treatment of patients (23).

Ultrasound

Ultrasound has been shown to have high sensitivity for interstitial-alveolar lung diseases with a peripheral distribution (31). It is a fast, feasible, and low-cost modality, which, in this outbreak, may play an important role in the diagnosis and triage of patients, and follow-up of disease progression, without the risk of contaminating the radiology department when performed using portable devices (16). A major advantage of ultrasound in COVID-19 pneumonia is its feasibility and efficacy owing to predilection of the disease for the peripheral subpleural areas (15, 16). However, lack of widespread experience in thoracic ultrasound has limited its use in this disease.

Chest CT in screening and diagnosis of COVID-19 pneumonia

Recent studies reported the sensitivity and specificity of CT in COVID-19 pneumo-

nia as 60%–98% and 25%–53%, respectively (23, 32–34). These wide ranges can be attributed to the retrospective design and relatively small sample size of the studies, variable imaging protocols, and the absence of definitive diagnostic criteria for imaging. The positive and negative predictive values of chest CT in COVID-19 pneumonia were found to be 92% and 42%, respectively, in a multicenter study in Chinese population (32). The low negative predictive value suggests that CT may not be suitable as a screening method in COVID-19 pneumonia, at least in the early stages of the disease. Sensitivity of CT depends on the time elapsed since the onset of symptoms. In a study of 121 symptomatic patients, a negative CT was found in 56% of patients scanned within two days of symptom onset, whereas negative scans were demonstrated in 9% and 4% of patients scanned within 3–5 days and 6–12 days of symptoms, respectively (22).

CT appears to have a higher sensitivity than rRT-PCR test. Long et al. (29) reported that initial CT sensitivity was 97.2%, while initial rRT-PCR test sensitivity was 83.3%. In

Main points

- Limitations of rRT-PCR test in the diagnosis of COVID-19 pneumonia, including relatively low sensitivity, availability issues, and long turnaround times have increased the role of imaging.
- Despite its lower sensitivity and specificity, portable radiography has been utilized in children, triage of outpatients, and follow-up of hospitalized patients.
- Though not recommended as a screening tool, chest CT has been widely employed in patients suspected for COVID-19 pneumonia, owing to its higher sensitivity compared with rRT-PCR test.
- Typical chest CT findings of COVID-19 pneumonia include bilateral, peripheral, ground glass opacities, and consolidations involving predominantly the lower lung lobes.
- Chest CT findings of COVID-19 pneumonia correlate with the disease severity and prognosis.

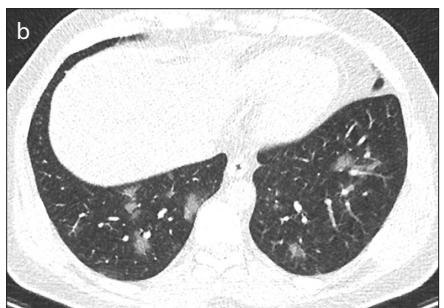
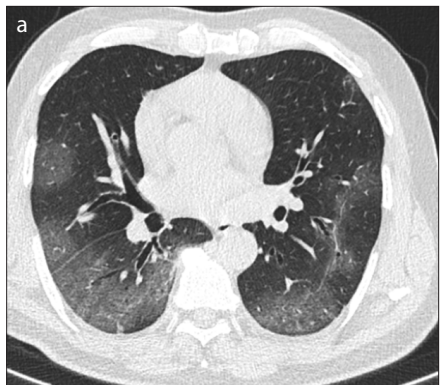


Figure 2. a, b. Findings typical for COVID-19 pneumonia. Axial CT image (a) shows bilateral confluent regions of GGO predominating in the peripheral parts of posterior lower lobes. Axial CT image (b) at the level of basis shows numerous round-shaped GGO in bilateral lower lobes.

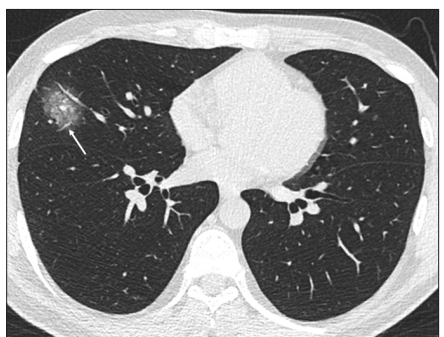


Figure 3. Axial CT image shows a focal, unilateral GGO (arrow) in the right lung of a patient with confirmed COVID-19 pneumonia.

line with this study, Fang et al. (34) reported that initial chest CT was more sensitive than initial rRT-PCR test in the early stages of the disease. CT was reported to become positive earlier than rRT-PCR test. Likewise, in the follow-up of patients, CT findings showed improvement earlier than rRT-PCR test becoming negative (23).

CT may even detect COVID-19 pneumonia in a small subset of asymptomatic patients (35). Additionally, it is a time-saving imaging modality compared with rRT-PCR test, which generally yields results in 5–6 hours (29).

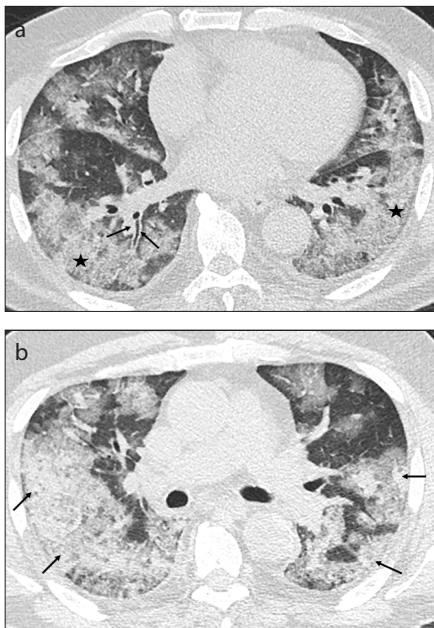


Figure 4. a, b. Axial CT image (a) shows bilateral consolidations (asterisks) and bronchial wall thickening (arrows) in the right lung. Axial CT image (b) shows bilateral consolidations (arrows).

CT findings of COVID-19 pneumonia overlap with many other infections (notably viral types of pneumonia) and noninfectious diseases (particularly organizing pneumonia). Bai et al. (21) stated that six of seven radiologists had high specificity, but moderate sensitivity in differentiation between COVID-19 and non-COVID viral pneumonia.

Despite its relatively high sensitivity, CT is generally not recommended in screening. Its use is mainly recommended to confirm the diagnosis of clinically suspected patients if the rRT-PCR test is negative or unavailable, in order to isolate and treat the patients quickly (14, 36).

CT findings

Demographic characteristics and CT findings of patients with COVID-19 pneumonia in 11 published articles are presented in the Table. The disease has a wide variety of CT features, which also depend on the clinical severity and the time elapsed since the onset of symptoms (24, 37). In the following sections, chest CT findings will be conveyed in three subheadings, namely the anatomic distribution of lesions, individual CT findings, and extrapulmonary features.

The anatomic distribution of lung lesions

Disease most commonly affects both lungs (82.2%), lower zones (54.5%), peripheral parts (87.1%), and multifocal ar-

eas (54.5%) (Fig. 2) (20). Another study confirmed this distribution and also found that posterior parts are involved in 80% of cases, and the disease is generally quite extensive, with all five lobes being affected in 39% of patients (5). Lower lobes are the most frequently involved lobes, and the right middle lobe is the least involved one (5, 8). Patchy multifocal distribution is more frequent compared with diffuse disease (20, 21); however, unilateral and even unifocal involvement can occur especially in early cases (Fig. 3). Exclusively peribronchial distribution, which was demonstrated only in 4% of patients, is considered so atypical that other diseases must be favored (18).

Reported CT findings

Ground glass opacity (GGO) is defined as a hazy hyperattenuated area without obscuration of the underlying vessels, and is typically caused by partial filling of the airspaces or interstitial thickening (Fig. 2) (38). COVID-19 pneumonia typically shows unilateral or bilateral GGO with peripheral and subpleural distribution (5, 39). GGO appears to be the most common CT finding, seen in up to 98% of patients (25, 40). Also, it is usually the earliest manifestation (12). It may or may not be accompanied by other findings, particularly consolidation and reticulation (5).

Consolidation is defined as a hyperattenuated area with obscuration of underlying vessels and is caused by complete filling of the alveolar airspaces (Fig. 4) (38). Multifocal, patchy, or segmental consolidations are present in COVID-19 pneumonia in 2%–64% of patients (18, 22, 25). Peripheral and subpleural lesions are more common compared with central peribronchovascular lesions (1, 18). Consolidations are generally patchy (1, 24), while round-shaped lesions were reported in 11%–54% of the patients (1, 22). Round lesions were considered relatively more specific to this disease (14). Consolidation usually appears later than GGO and peaks in days 10–12 after the onset of the disease (37).

Reticulation is defined as thickened interlobular septa and intralobular lines which appear as linear opacities on CT (Fig. 5) (38, 41). Reticulation was found to be the third most common CT appearance following GGO and consolidation, with a rate of 48.5%–59% (18, 20). Compared with GGO and consolidation, it is a relatively late finding (24).

Crazy-paving pattern is defined as thickened interlobular septa or intralobular lines superimposed on GGO, resembling paving

Table. Demographics and chest CT findings of the patients with COVID-19 pneumonia (according to 11 published studies with a sample size of more than 50 patients)

| | Han (1) | Song (5) | Wu (18) | Li Y. (19) | Zhao (20) | Bai (21) | Bernheim (22) | Ai (23) | Shi (24) | Li K. (25) | Guan (26) |
|----------------------------------|------------|-------------|------------|---------------|--------------|-------------|------------------|------------|-------------|---------------|--------------|
| Patients' demographics | | | | | | | | | | | |
| Number of patients, n | 108 | 51 | 80 | 51 | 101 | 219 | 121 | 1014 | 81 | 83 | 1099 |
| Median age (years) | 45 | 49 | 44 | 58 | 44 | 45 | 45 | 51 | 50 | 46 | 47 |
| Male, n | 38 | 25 | 42 | 28 | 56 | 119 | 61 | 467 | 42 | 44 | 637 |
| Distribution of lesions | | | | | | | | | | | |
| Normal CT (%) | 0 | 0 | | 4 | 8 | | 22 | 12 | 0 | | 14 |
| Bilateral/Unilateral (%) | | | 86/14 | | | 82/10 | 75/19 | 60/18 | 79/21 | 95/5 | 52/34 |
| Peripheral/Central (%) | 90/2 | 86/10 | 53/NA | 96/NA | 87/1 | 80/1 | 52/0 | | 54/NA | | |
| Multifocal/Diffuse (%) | | | NA/9 | | 55/32 | 61/27 | | | NA/44 | | |
| 1 lobe/5 lobes involvement (%) | 35/NA | 8/39 | | NA/75 | | | 15/27 | | | | |
| Right upper/Left upper lobes (%) | | | | | | | 44/48 | | 19/20 | 65/86 | |
| Middle lobe (%) | | | | | | | 41 | | 10 | 74 | |
| Right lower/Left lower lobes (%) | | | 84/79 | | | | 65/63 | | 27/24 | 94/96 | |
| CT appearances of lesions | | | | | | | | | | | |
| GGO (%) | 60 | 77 | 91 | 35 | 86 | 91 | 34 | 46 | 65 | 98 | 56 |
| Consolidation (%) | 6 | 55 | 63 | 6 | 44 | 69 | 2 | 50 | 17 | 64 | |
| GGO and consolidation (%) | 41 | 59 | | 55 | 64 | | 41 | | | | |
| Reticulation (%) | | 22 | 59 | | 49 | 35 | 7 | 1 | 35 | | |
| CT signs | | | | | | | | | | | |
| Crazy paving pattern (%) | 40 | | 29 | 71 | | 5 | 5 | | 10 | 36 | |
| Spider web sign (%) | | | 25 | | | | | | | 25 | |
| Air bronchogram (%) | 48 | 80 | | 69 | | 14 | | | 47 | | |
| Bronchiectasis (%) | | | | | 53 | | 1 | | 11 | | |
| Bronchial wall thickening (%) | | | 11 | | 29 | 9 | 12 | | | 23 | |
| Subpleural line (%) | | | 20 | | 28 | | | | | 21 | |
| Vascular enlargement (%) | 80 | | | 82 | 71 | 59 | | | | | |
| Halo sign (%) | 64 | | | 18 | | 26 | | | | | |
| Reversed halo sign (%) | | | | 4 | | 5 | 2 | | | | |
| Nodules (%) | | | | 22 | 23 | 32 | 0 | 3 | 6 | 7 | |
| Extrapulmonary findings | | | | | | | | | | | |
| Pleural effusion (%) | 0 | 8 | 6 | 2 | 14 | 4 | 1 | | 5 | 8 | |
| Pleural thickening (%) | 0 | | | | | 15 | | | 32 | | |
| Lymphadenopathy (%) | 0 | 6 | 4 | 0 | 1 | 3 | 0 | | 6 | 8 | |
| Pericardial effusion (%) | | 6 | 5 | | | | | | | 5 | |

CT, computed tomography; COVID-19, coronavirus disease 2019; GGO, ground glass opacities; NA, not applicable.

stones (Fig. 6) (37, 38). This sign may refer to the alveolar edema and acute interstitial inflammation presented also in severe acute respiratory syndrome (SARS) (18, 42). It was reported in 5%–36% of patients with COVID-19 pneumonia (22, 25). Spider web sign, which was first defined in this disease, showed a triangular or angular GGO under

the pleura including thickened interlobular septa resembling a net (18).

Air bronchogram, defined as visible bronchial lumina in a hyperattenuated area, has been variably reported in 28%–80% of patients (Fig. 7) (5, 28, 38).

Air trapping is a rare finding that was reported in only one study in 12% of patients (19).

Bronchiectasis and bronchial wall thickening may also be seen in COVID-19 pneumonia (Fig. 8) (18, 22, 25). Bronchial wall thickening was found more commonly in clinically severe/critical patients (25). It may be more frequent in other types of viral pneumonia compared with COVID-19 pneumonia (21). Traction bronchiectasis

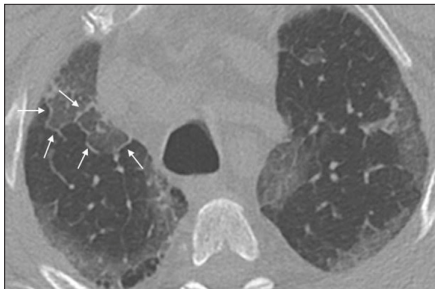


Figure 5. Axial CT image shows thickened interlobular septa (arrows) delineating secondary pulmonary lobules in the right lung.

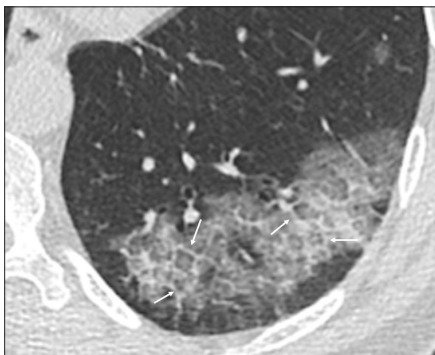


Figure 6. Axial CT image shows thickened interlobular septa (arrows) superimposed on a background of ground glass attenuation showing a crazy paving pattern. A barely discernible finer reticular pattern formed by thickened intralobular interstitium is also noted.

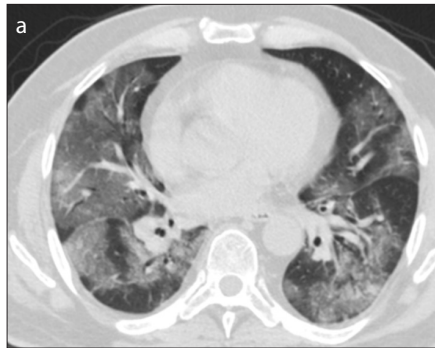


Figure 8. a, b. Axial CT image (a) shows bilateral GGO. Axial CT image after one month (b) shows resorption of GGO, development of band-shaped, irregular fibrotic opacities with traction bronchiectasis (arrows) and a large bulla (asterisk). Note the predilection of fibrosis for the anterior parts of lungs.



Figure 9. Axial CT image shows bilateral, subpleural, linear and curvilinear lines (arrows) located posteriorly, close to the pleura.



Figure 7. Axial CT image shows bilateral consolidation with an air bronchogram (arrow) in the left lung.

was observed in 53% of patients in a study (20), which was relatively higher than those reported in other studies.

Fibrosis is defined as lung scarring reflected as reticular changes associated with interstitial thickening, traction bronchiectasis, clusters of subpleural cystic airspaces, and decrease in lung volume (43). Two studies reported the presence of fibrosis in 17%–20% of patients (19, 39). The impact of fibrosis on prognosis is controversial. While it has been suggested to indicate recovery

and good prognosis, others claim that it is a poor prognostic sign (37, 39, 44, 45).

Subpleural curvilinear line is defined as a thin, curvilinear-shaped opacity with 1–3 mm thickness, seen in close proximity to the pleural surface (Fig. 9) (38). Thought to reflect pulmonary edema or fibrosis, this finding has been found in approximately 20% of patients (18, 25).

Architectural distortion is defined when the normal pulmonary anatomy is disrupted and manifests as loss of smooth course of the fissures, crowding of dilated bronchioles or vessels with angulated course (38). It was reported in 21.8% of 101 patients in the study of Zhao et al. (20).

Among the relatively more specific signs, vascular enlargement denotes the dilatation of pulmonary vessels within the lesions, especially in GGO (Fig. 10) (44). It is a quite common sign, having been reported in 71.3%–82.4% of patients (19, 20).

Halo sign is defined as nodules or masses surrounded by GGO (38). It has been demonstrated in a variety of disease processes, including the angioinvasive fungal infections, viral infections, organizing pneumonia, and



hypervascular metastases, among others (Fig. 11a) (46, 47). Reversed halo sign, also known as atoll sign, refers to a focal round GGO surrounded by complete or incomplete ring-like consolidation (Fig. 11b) (38). Although considered pathognomonic for cryptogenic organizing pneumonia initially (48), it has later proved a rather nonspecific finding that can be seen in many other diseases (49). Recent studies showed that this sign can be present in COVID-19 patients and may reflect an absorption within the lesion (2, 28, 50). Reportedly, a halo occurs in 18%–64% (1, 19, 21), whereas a reversed halo is seen in 2%–5% (19, 21, 22) of patients.

Relatively rare findings include the air bubble sign and nodules (20, 24). The air bubble sign refers to an air-containing, well-defined lucency in the lung (Fig. 12). It was reported as cystic change (24) or cavity (45), and the incidence was reported as 10% in the study of Shi et al. (24). Nodules were reported in 3%–13% of patients with COVID-19 pneumonia (23, 51), which was less than that seen in other types of viral pneumonia (52). The “tree-in-bud”, first described in patients with endobronchial tuberculosis, refers to multiple centrilobular nodules with a linear branching pattern (53). As it has not been reported in patients with COVID-19 pneumonia (20, 24), this sign may indicate the presence of other infectious diseases.

A perilobular pattern, which is well known in organizing pneumonia, can also be seen in COVID-19 pneumonia (54, 55). Arcade-like or polygonal curvilinear opacities representing the perilobular pattern can be seen in some patients with COVID-19 pneumonia (Fig. 13).

Extrapulmonary findings

Pleural thickening is not rare, being reported in 32 of patients, but pleural

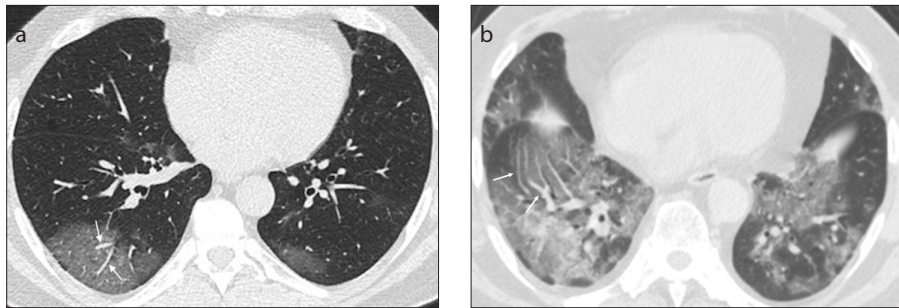


Figure 10. a, b. Axial CT image (a) reveals increased caliber of vessels (arrows) within the GGO, compared with vessels in the adjacent normal lung. Axial CT image (b) reveals increase in the number of vessels and enlargement of vessels (arrows) within GGO.

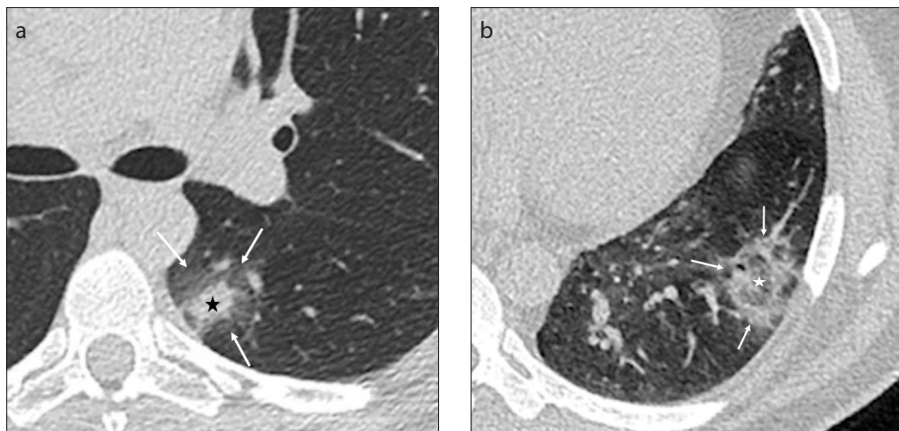


Figure 11. a, b. Axial CT image (a) reveals a ground glass halo (arrows) surrounding a denser nodule (asterisk). Axial CT image (b) reveals a reversed halo formed by a dense ring (arrows) encircling a central area of GGO (asterisk).



Figure 12. Axial CT image reveals an extensive GGO representing diffuse alveolar damage. Note the presence of two small, well-defined foci of lucency (arrows) in the right lung.

effusion is rather infrequent, seen in less than 5% of patients (22, 24). As is the case with Middle East Respiratory Syndrome Coronavirus (MERS-CoV) infection, the presence of pleural effusion may indicate a poor prognosis also in COVID-19 pneumonia (24, 25). Additionally, a combination of extensive tiny nodules and pleural

effusion may suggest bacterial superinfection (56).

Pericardial effusion is rare in COVID-19 patients, with an incidence of approximately 5% (18, 25). However, it was thought to be associated with severe disease (25).

Enlarged mediastinal lymph nodes exceeding 1 cm in short axis diameter was reported in 4%–8% of patients with COVID-19 pneumonia (18, 24, 38). Like pleural and pericardial effusions, lymphadenopathy was also considered an indicator for severe disease (25).

CT reporting standardization

In the classification of RSNA expert consensus statement, chest CT findings of COVID-19 pneumonia were classified in four categories (14). The first category, referred to as typical findings, include peripheral, bilateral GGO or multifocal GGO of rounded morphology with or without consolidation or visible intralobular lines (crazy-paving pattern), and reverse halo sign or other findings of organizing pneumonia (Fig. 2) (14, 21, 55, 57). These include

the commonly reported imaging findings of greater specificity for COVID-19 pneumonia. The second category, namely the indeterminate findings, include the absence of typical findings and the presence of non-specific findings such as non-rounded or non-peripheral multifocal, diffuse, perihilar, or unilateral GGO with or without consolidation lacking a specific distribution and a few very small GGOs with a non-rounded and non-peripheral distribution (Figs. 3, 14). These findings may be seen with COVID-19 pneumonia, but they are regarded as non-specific for this disease. The third category (atypical findings) include the absence of typical or indeterminate findings and the presence of isolated lobar or segmental consolidation without GGO, discrete small nodules (centrilobular, tree-in-bud pattern), lung cavitation, and smooth interlobular septal thickening with pleural effusion (Fig. 15). These are either uncommon or not reported in COVID-19 pneumonia. The fourth category (negative for pneumonia) denotes the situation in which there are no findings for pneumonia. It must be stressed that chest CT can be normal in the early stages of COVID-19 pneumonia (8, 14).

Changes in CT with time and correlation with clinical severity

Pan et al. (37) stated that there are four stages of COVID-19 pneumonia. In the early stage (i.e., 0–4 days after the onset of symptoms), nodular or patchy subpleural GGO in the lower lobes either uni- or bilaterally was the main finding (58, 59). Vascular enlargement and the halo sign may be seen in this stage (22, 56). In the progressive stage, typically 5–8 days after the onset of the symptoms, disease extends to a bilateral and multilobar distribution with diffuse GGO, consolidation, and crazy-paving pattern (12, 60). New lesions, lesions with partial absorption, architectural distortion, bronchial wall thickening, and focal atelectasis may also be seen. In the peak stage, 9–13 days after the onset of the symptoms, massive consolidations, diffuse GGO, parenchymal bands, and crazy-paving predominate. Grossly the lungs appear “white” in this severe stage. Air bronchograms, loss of volume, and mild pleural effusion may also be seen. In the absorption stage, later than 14 days after the onset of the symptoms, consolidation and crazy-paving leave their place to fibrosis and extensive GGO (37).

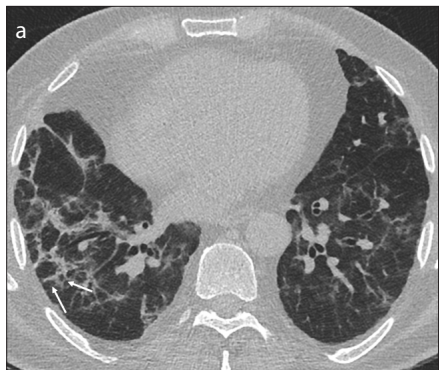


Figure 13. a, b. Perilobular opacities. Axial CT image (a) reveals numerous, subpleural, arcade-shaped opacities (arrows) in the right lung. Axial CT image (b) revealing perilobular opacities (arrows).

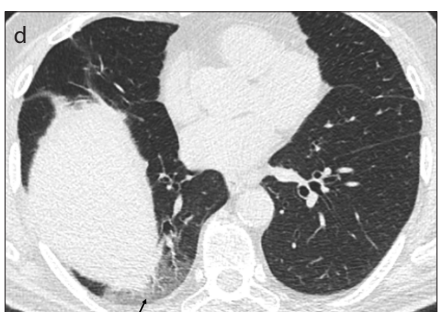


Figure 14. a-d. Two patients with indeterminate findings. Axial CT image (a) shows non-rounded opacities located predominantly in central peribronchovascular regions. Axial CT image (b) of the same patient showing central, peribronchovascular opacities. Axial CT image (c) of another patient reveals a GGO (arrow) in the right upper lobe. Axial CT image (d) of the same patient revealing a GGO (arrow) in the right lower lobe. The left lung was entirely normal.

Regarding the use of serial CTs in the follow-up of patients, they should be performed in selected cases with suspected complications, e.g., superinfection and pulmonary embolism, especially in patients requiring supplemental oxygen. Repeat scans should not be used routinely in clinically stable patients.

The extent of parenchymal involvement on CT, as assessed by semiquantitative methods, has been shown to correlate with the clinical severity of disease and the need for intensive care (8, 12, 61). Patients with more widespread disease and relatively higher proportion of consolidation have a worse prognosis and higher mortality (62). Semiquantitative scores of severe to critical

patients were found to be higher. Severe to critical patients more commonly showed involvement of all five lobes (8).

Artificial intelligence

Artificial intelligence (AI) has high sensitivity and specificity in the diagnosis of both COVID-19 pneumonia and community-acquired pneumonia, and a machine learning approach using convolutional networks model could distinguish COVID-19 from community-acquired pneumonia (63). Additionally, involved lung areas can be detected with AI, and the volume of involved areas can be more accurately calculated compared with the visual semiquantitative methods. This volumetric calculation

reflects the extension of the disease and it can be used in the prediction of the severity, progression, and treatment response of the disease (64).

The role of radiology in unusual presentations

Gastrointestinal symptoms, notably diarrhea, can be the sole manifestation both in children and adults, and they are more common in the later stages of the disease (6). In an era of COVID-19 outbreak, it is advisable to examine carefully the basal lung regions for possible pneumonia in abdominal CT scans.

A case of acute myopericarditis with fatigue has been presented without any interstitial pneumonia (65). There were diffuse ST elevations on electrocardiography and elevated levels of cardiac enzymes mimicking myocardial infarction. The patient had no obstructive cardiac disease on angiography, whereas he had increased wall thickness with ventricular hypokinesis, myocardial interstitial edema, diffuse late gadolinium enhancement, and pericardial effusion demonstrated on cardiac MRI.

Acute necrotizing encephalopathy, caused by intracranial cytokine storm, was reported as a rare complication of COVID-19 (7, 66).

Differentiation from other types of pneumonia

Chest CT findings of COVID-19 pneumonia in children are similar to those in adults, and most of the children have clinically mild to moderate symptoms (5, 56). The typical appearances were consolidations with surrounding halo sign in nearly 50% of patients and unilateral or bilateral subpleural GGO (67). COVID-19 pneumonia should be distinguished from other types of pneumonia, such as those caused by influenza virus, parainfluenza virus, respiratory syncytial virus, and adenovirus (68). In adenovirus, mycoplasma, and chlamydia pneumonia, consolidations with higher density are present. Additionally, adenovirus pneumonia tends to involve subpleural areas to a lesser degree compared with COVID-19 pneumonia (67). Lesions due to respiratory syncytial virus and parainfluenza virus pneumonia generally show peribronchial distribution with bronchial wall thickening, and influenza virus demonstrates grid-like changes in the lungs, which were reported rarely in COVID-19 pneumonia (67).

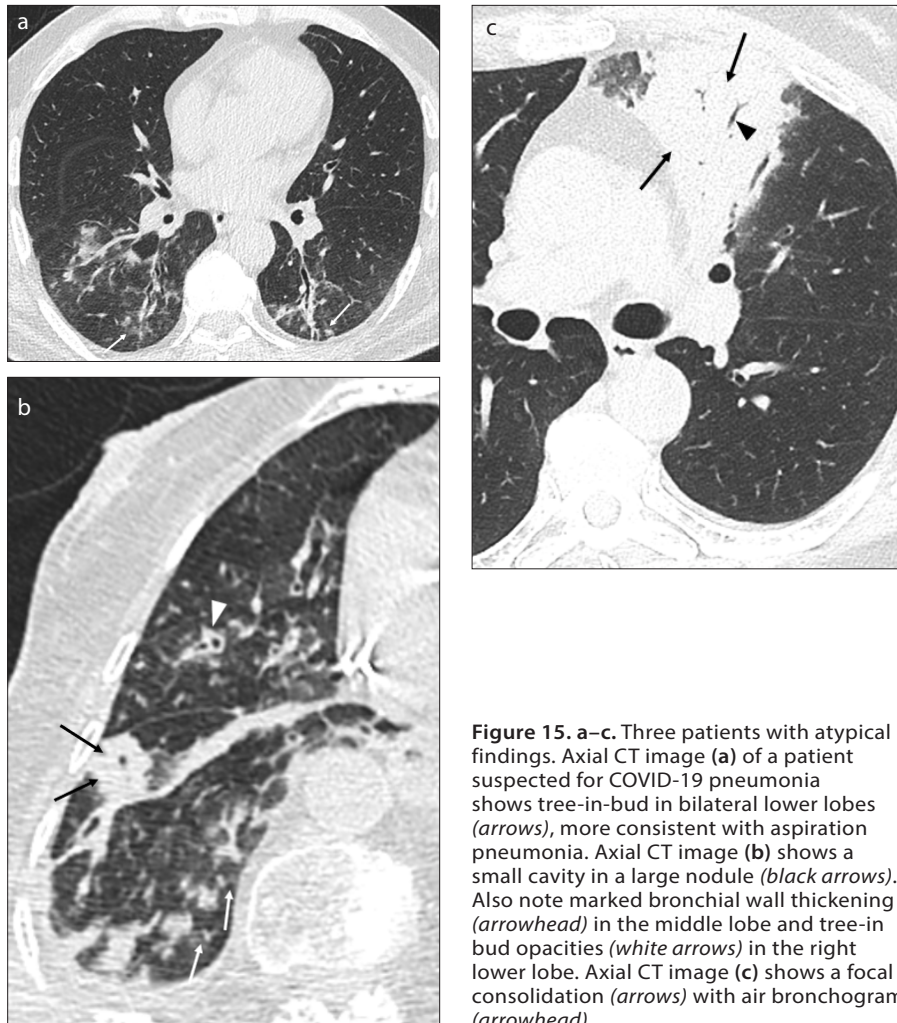


Figure 15. a–c. Three patients with atypical findings. Axial CT image (a) of a patient suspected for COVID-19 pneumonia shows tree-in-bud in bilateral lower lobes (arrows), more consistent with aspiration pneumonia. Axial CT image (b) shows a small cavity in a large nodule (black arrows). Also note marked bronchial wall thickening (arrowhead) in the middle lobe and tree-in bud opacities (white arrows) in the right lower lobe. Axial CT image (c) shows a focal consolidation (arrows) with air bronchogram (arrowhead).

In adults, findings of SARS-CoV-2 pneumonia may be similar to those of adenovirus, SARS-CoV and MERS-CoV (19). Li et al. (19) reported two patients with adenovirus pneumonia presenting with subpleural GGO and consolidation that mimicked COVID-19 pneumonia. A reversed halo sign was present in 3.9% and a halo sign in 17.6% of patients with COVID-19 pneumonia, which were not reported in patients with SARS and MERS (19). Compared with COVID-19 disease, unifocal involvement is more common in patients with SARS and MERS (69, 70). However, progression to upper lobes and central areas may occur in SARS, MERS, and COVID-19, which makes the differentiation difficult (69, 70).

Although RSNA expert consensus statement defined the “typical” findings for COVID-19 pneumonia that have a relatively high specificity, it must be noted that similar findings may be seen in a variety of other pneumonia types and non-infec-

tious diseases. On the other hand, patients with COVID-19 pneumonia may have the so called “indeterminate” and “atypical” findings (14, 19). Thus, the definitive differentiation between different causes of pneumonia is still not possible based only on CT, and should rely upon virologic identification of the causative agent.

Conclusion

Radiology has been used effectively in COVID-19 outbreak, and chest CT has taken a big share among all imaging modalities. Because a relatively short period of time elapsed since the outset of the pandemic, knowledge on the imaging features and the role of radiology in the diagnostic algorithm is still evolving. The use of chest CT in screening is still controversial due to a relatively wide range of reported sensitivity rates, but it has been widely used in the diagnosis and clinical

management almost worldwide, particularly at settings where the availability and accuracy of virologic identification have been questionable. Although a typical constellation of findings favors the disease with a reasonably high specificity, other infectious and noninfectious processes may result in quite similar appearances. A normal chest CT can negate the diagnosis in an overwhelming majority of patients, particularly when performed a couple of days after the onset of symptoms.

Conflict of interest disclosure

The authors declared no conflicts of interest.

References

1. Han R, Huang L, Jiang H, Dong J, Peng H, Zhang D. Early Clinical and CT manifestations of coronavirus disease 2019 (COVID-19) pneumonia. *AJR Am J Roentgenol* 2020; 1–6. [\[Crossref\]](#)
2. Chen N, Zhou M, Dong X, et al. Epidemiological and clinical characteristics of 99 cases of 2019 novel coronavirus pneumonia in Wuhan, China: a descriptive study. *Lancet* 2020; 395:507–513. [\[Crossref\]](#)
3. Li Q, Guan X, Wu P, et al. Early transmission dynamics in Wuhan, China, of novel coronavirus-infected pneumonia. *N Eng J Med* 2020; 382:1199–1207. [\[Crossref\]](#)
4. Chu DKW, Pan Y, Cheng SMS, et al. Molecular diagnosis of a novel coronavirus (2019-nCoV) causing an outbreak of pneumonia. *Clin Chem* 2020; 66:549–555. [\[Crossref\]](#)
5. Song F, Shi N, Shan F, et al. Emerging 2019 novel coronavirus (2019-nCoV) pneumonia. *Radiology* 2020; 295:210–217. [\[Crossref\]](#)
6. Tian Y, Rong L, Nian W, He Y. Review article: gastrointestinal features in COVID-19 and the possibility of faecal transmission. *Aliment Pharmacol Ther* 2020; 51:843–851. [\[Crossref\]](#)
7. Poyiadji N, Shahin G, Noujaim D, Stone M, Patel S, Griffith B. COVID-19-associated acute hemorrhagic necrotizing encephalopathy: CT and MRI features. *Radiology* 2020 Mar 31. [Epub ahead of print] [\[Crossref\]](#)
8. Li K, Fang Y, Li W, et al. CT image visual quantitative evaluation and clinical classification of coronavirus disease (COVID-19). *Eur Radiol* 2020 Mar 25. [Epub ahead of print] [\[Crossref\]](#)
9. Corman VM, Landt O, Kaiser M, et al. Detection of 2019 novel coronavirus (2019-nCoV) by real-time RT-PCR. *Euro Surveill* 2020; 25:2000045. [\[Crossref\]](#)
10. Rubin EJ, Baden LR, Morrissey S, Campion EW. Medical journals and the 2019-nCoV outbreak. *N Engl J Med*. 2020; 382:866. [\[Crossref\]](#)
11. Loeffelholz MJ, Tang YW. Laboratory diagnosis of emerging human coronavirus infections – the state of the art. *A Emerg Microbes Infect* 2020; 20:1–26. [\[Crossref\]](#)
12. Chung M, Bernheim A, Mei X, et al. CT imaging features of 2019 novel coronavirus (2019-nCoV). *Radiology* 2020; 295:202–207. [\[Crossref\]](#)
13. Pan Y, Guan H. Imaging changes in patients with 2019-nCoV. *Eur Radiol* 2020; 1–2. [\[Crossref\]](#)

14. Simpson S, Kay FU, Abbara S, et al. Radiological Society of North America expert consensus statement on reporting chest CT findings related to COVID-19. Endorsed by the Society of Thoracic Radiology, the American College of Radiology, and RSNA. *Radiology* 2020 Mar 25. [Epub ahead of print] [\[Crossref\]](#)
15. Wong HYF, Lam HYS, Fong AH, et al. Frequency and distribution of chest radiographic findings in COVID-19 positive patients. *Radiology* 2019 Mar 27. [Epub ahead of print] [\[Crossref\]](#)
16. Soldati G, Smargiassi A, Inchegolo R, et al. Is there a role for lung ultrasound during the COVID-19 pandemic? *J Ultrasound Med* 2020 Mar 20. [Epub ahead of print] [\[Crossref\]](#)
17. Zou S, Zhu X. FDG PET/CT of COVID-19. *Radiology* 2020 Mar 6. [Epub ahead of print] [\[Crossref\]](#)
18. Wu J, Wu X, Zeng W, et al. Chest CT findings in patients with coronavirus disease 2019 and its relationship with clinical features. *Invest Radiol* 2020; 55:257–261. [\[Crossref\]](#)
19. Li Y, Xia L. Coronavirus disease 2019 (COVID-19): role of chest CT in diagnosis and management. *AJR Am J Roentgenol* 2020; 1–7. [\[Crossref\]](#)
20. Zhao W, Zhong Z, Xie X, Yu Q, Liu J. Relation between chest CT findings and clinical conditions of coronavirus disease (COVID-19) pneumonia: a multicenter study. *AJR Am J Roentgenol* 2020; 1–6. [\[Crossref\]](#)
21. Bai HX, Hsieh B, Xiong Z, et al. Performance of radiologists in differentiating COVID-19 from viral pneumonia on chest CT. *Radiology* 2020 Mar 10. [Epub ahead of print] [\[Crossref\]](#)
22. Bernheim A, Mei X, Huang M, et al. Chest CT findings in coronavirus disease-19 (COVID-19): relationship to duration of infection. *Radiology* 2020 Feb 20. [Epub ahead of print] [\[Crossref\]](#)
23. Ai T, Yang Z, Hou H, et al. Correlation of chest CT and RT-PCR testing in coronavirus disease 2019 (COVID-19) in China: A report of 1014 cases. *Radiology* 2020 Feb 26. [Epub ahead of print] [\[Crossref\]](#)
24. Shi H, Han X, Jiang N, et al. Radiological findings from 81 patients with COVID-19 pneumonia in Wuhan, China: a descriptive study. *Lancet Infect Dis* 2020; 20:425–434. [\[Crossref\]](#)
25. Li K, Wu J, Wu F, et al. The clinical and chest CT features associated with severe and critical COVID-19 pneumonia. *Invest Radiol* 2020 Feb 29. [Epub ahead of print] [\[Crossref\]](#)
26. Guan WJ, Ni ZY, Hu Y, et al. Clinical characteristics of coronavirus disease 2019 in China. *N Engl J Med* 2020 Feb 28. [Epub ahead of print]
27. ACR Recommendations for the use of chest radiography and computed tomography (CT) for suspected COVID-19 infection. Available at: <https://www.acr.org/Advocacy-and-Economics/ACR-Position-Statements/Recommendations-for-Chest-Radiography-and-CT-for-Suspected-COVID19-Infection>. Accessed March 11, 2020.
28. Yoon SH, Lee KH, Kim JY, et al. Chest radiographic and CT findings of the 2019 novel coronavirus disease (COVID-19): analysis of nine patients treated in Korea. *Korean J Radiol* 2020; 21:494–500. [\[Crossref\]](#)
29. Long C, Xu H, Shen Q, et al. Diagnosis of the coronavirus disease (COVID-19): rRT-PCR or CT? *Eur J Radiol* 2020; 126:108961. [\[Crossref\]](#)
30. Rubin GD, Ryerson CJ, Haramati LB, et al. The role of chest imaging in patient management during the COVID-19 pandemic: a multinational consensus statement from the Fleischner Society Radiology 2020 Apr 7. [Epub ahead of print] [\[Crossref\]](#)
31. Bass CM, Sajed DR, Adedipe AA, West TE. Pulmonary ultrasound and pulse oximetry versus chest radiography and arterial blood gas analysis for the diagnosis of acute respiratory distress syndrome: a pilot study. *Crit Care* 2015; 19:282. [\[Crossref\]](#)
32. Wen Z, Chi Y, Zhang L, et al. Coronavirus disease 2019: initial detection on chest CT in a retrospective multicenter study of 103 Chinese subjects. *RYCT-20-0092*, in press.
33. Inui S, Fujikawa A, Jitsu M, et al. Chest CT findings in cases from the cruise ship "Diamond Princess" with coronavirus disease 2019 (COVID-19). *Radiology* 2020 Mar 17. [Epub ahead of print] [\[Crossref\]](#)
34. Fang Y, Zhang H, Xie J, et al. Sensitivity of chest CT for COVID-19: comparison to RT-PCR. *Radiology* 2020; 19:200432. [\[Crossref\]](#)
35. Lee EYP, Ng MY, Khong PL. COVID-19 pneumonia: what has CT taught us?. *Lancet Infect Dis* 2020; 20:384–385. [\[Crossref\]](#)
36. Xie X, Zhong Z, Zhao W, Zheng C, Wang F, Liu J. Chest CT for typical 2019-nCoV pneumonia: relationship to negative RT-PCR testing. *Radiology* 2020 Feb 1. [Epub ahead of print] [\[Crossref\]](#)
37. Pan F, Ye T, Sun P, et al. Time course of lung changes on chest CT during recovery from 2019 novel coronavirus (COVID-19) pneumonia. *Radiology* 2020 Feb 13. [Epub ahead of print] [\[Crossref\]](#)
38. Hansell DM, Bankier AA, MacMahon H, McLoud TC, Müller NL, Remy J. Fleischner Society: glossary of terms for thoracic imaging. *Radiology* 2008; 246:697–722. [\[Crossref\]](#)
39. Pan Y, Guan H, Zhou S, et al. Initial CT findings and temporal changes in patients with the novel coronavirus pneumonia (2019-nCoV): a study of 63 patients in Wuhan, China. *Eur Radiol* 2020 Feb 13. [Epub ahead of print] [\[Crossref\]](#)
40. Hamer OW, Salzberger B, Gebauer J, Stroszczynski C, Pfeifer M. CT morphology of COVID-19: Case report and review of literature. *Rofo* 2020 Mar 26. [Epub ahead of print] [\[Crossref\]](#)
41. Ajlan AM, Ahyad RA, Jamjoom LG, Alharthy A, Madani TA. Middle East respiratory syndrome coronavirus (MERS-CoV) infection: chest CT findings. *AJR Am J Roentgenol* 2014; 203:782–787. [\[Crossref\]](#)
42. Wong K, Antonio GE, Hui DS, et al. Thin-section CT of severe acute respiratory syndrome: evaluation of 73 patients exposed to or with the disease. *Radiology* 2003; 228:395–400. [\[Crossref\]](#)
43. Martinez FJ, Collard HR, Pardo A, et al. Idiopathic pulmonary fibrosis. *Nat Rev Dis Primers* 2017; 3:17074. [\[Crossref\]](#)
44. Ye Z, Zhang Y, Wang Y, Huang Z, Song B. Chest CT manifestations of new coronavirus disease 2019 (COVID-19): a pictorial review. *Eur Radiol* 2020 Mar 19. [Epub ahead of print] [\[Crossref\]](#)
45. Kong W, Agarwal PP. Chest imaging appearance of COVID-19 infection. *Radiology* 2020 Feb 13. [Epub ahead of print] [\[Crossref\]](#)
46. Kuhlman JE, Fishman EK, Siegelman S. Invasive pulmonary aspergillosis in acute leukemia: characteristic findings on CT, the CT halo sign, and the role of CT in early diagnosis. *Radiology* 1985; 157:611–614. [\[Crossref\]](#)
47. Pinto PS. The CT halo sign. *Radiology* 2004; 230:109–110. [\[Crossref\]](#)
48. Kim SJ, Lee KS, Ryu YH, et al. Reversed halo sign on high resolution CT of cryptogenic organizing pneumonia: diagnostic implications. *AJR Am J Roentgenol* 2003; 180:1251–1254. [\[Crossref\]](#)
49. Gasparetto EL, Escuissato DL, Davaus T, et al. Reversed halo sign in pulmonary paracoccidioidomycosis. *AJR Am J Roentgenol* 2005; 184:1932–1934. [\[Crossref\]](#)
50. Huang P, Liu T, Huang L, et al. Use of chest CT in combination with negative RT-PCR assay for the 2019 novel coronavirus but high clinical suspicion. *Radiology* 2020; 295:22–23. [\[Crossref\]](#)
51. Li X, Zeng X, Liu B, Yu Y. COVID-19 infection presenting with CT halo sign. *Radiology* 2020 Feb 12. [\[Crossref\]](#)
52. Franquet T. Imaging of pulmonary viral pneumonia. *Radiology* 2011; 260:18–39. [\[Crossref\]](#)
53. Eisenhuber E. The tree-in-bud sign. *Radiology* 2002; 222:771–772. [\[Crossref\]](#)
54. Mehrjardi MZ, Kahkouee S, Pourabdollah M. Radio-pathological correlation of organizing pneumonia (OP): a pictorial review. *Br J Radiol* 2017; 90:20160723. [\[Crossref\]](#)
55. Hani C, Trieu NH, Saab I, et al. COVID-19 pneumonia: A review of typical CT findings and differential diagnosis. *Diagn Interv Imaging* 2020; S2211-5684:30091–30097. [\[Crossref\]](#)
56. Kanne JP, Little BP, Chung JH, Elicker BM, Ketai LH. Essentials for radiologists on COVID-19: an update- Radiology Scientific Expert Panel. *Radiology* 2020 Feb 27. [Epub ahead of print] [\[Crossref\]](#)
57. Salehi S, Abedi A, Balakrishnan S, Gholamrezaeezad A. Coronavirus disease 2019 (COVID-19): a systematic review of imaging findings in 919 patients. *AJR Am J Roentgenol* 2020; 1–7. [\[Crossref\]](#)
58. Kim JY, Ko JH, Kim Y, et al. Viral load kinetics of SARS-CoV-2 infection in first two patients in Korea. *J Korean Med Sci* 2020; 35:e86. [\[Crossref\]](#)
59. Lin X, Gong Z, Xiao Z, Xiong J, Fan B, Liu J. Novel coronavirus pneumonia outbreak in 2019: computed tomographic findings in two cases. *Korean J Radiol* 2020; 21:365–368. [\[Crossref\]](#)
60. Lei J, Li J, Li X, Qi X. CT Imaging of the 2019 novel coronavirus (2019-nCoV) pneumonia. *Radiology* 2020; 295:18. [\[Crossref\]](#)
61. Li M, Lei P, Zeng B, et al. Coronavirus disease (COVID-19): spectrum of CT findings and temporal progression of the disease. *Acad Radiol* 2020; S1076-6332:30144–30146.
62. Yuan M, Yin W, Tao Z, Tan W, Hu Y. Association of radiologic findings with mortality of patients infected with 2019 novel coronavirus in Wuhan, China. *PLoS One* 2020; 15:e0230548. [\[Crossref\]](#)
63. Li L, Qin L, Xu Z, et al. Artificial intelligence distinguishes COVID-19 from community acquired pneumonia on chest CT. *Radiology* 2020 Mar 19. [Epub ahead of print] [\[Crossref\]](#)

64. Long JB, Ehrenfeld JM. The role of augmented intelligence (AI) in detecting and preventing the spread of novel coronavirus. *J Med Syst* 2020; 44:59. [\[Crossref\]](#)
65. Inciardi RM, Lupi L, Zaccone G, et al. Cardiac involvement in a patient with coronavirus disease 2019 (COVID-19). *Cardiol* 2020 Mar 27. [Epub ahead of print] [\[Crossref\]](#)
66. Mehta P, McAuley DF, Brown M, Sanchez E, Tattersall RS, Manson JJ. COVID-19: consider cytokine storm syndromes and immunosuppression. *Lancet* 2020; 395:1033–1034. [\[Crossref\]](#)
67. Xia W, Shao J, Guo Y, Peng X, Li Z, Hu D. Clinical and CT features in pediatric patients with COVID-19 infection: Different points from adults. *Pediatr Pulmonol* 2020; 55:1169–1174. [\[Crossref\]](#)
68. Virkki R, Juven T, Rikalainen H, Svedstrom E, Mertsola J, Ruuskanen O. Differentiation of bacterial and viral pneumonia in children. *Thorax* 2002; 57:438–441. [\[Crossref\]](#)
69. Das KM, Lee EY, Langer RD, Larsson SG. Middle East respiratory syndrome coronavirus: what does a radiologist need to know? *AJR Am J Roentgenol* 2016; 206:1193–1201. [\[Crossref\]](#)
70. Paul NS, Roberts H, Butany J, et al. Radiologic pattern of disease in patients with severe acute respiratory syndrome: the Toronto experience. *Radiographics* 2004; 24:553–563. [\[Crossref\]](#)